Available online at www.sciencedirect.com
ScienceDirect
Journal of Organometallic Chemistry 693 (2008) 1065–1072
Journal of Organometallic Chemistry
www.elsevier.com/locate/jorganchem

Synthesis, characterization, and spectrophotometric studies of novel fluorescent *arachno* decaborane and nonaborane clusters containing aza-distyrylbenzene derivatives

Afaf R. Genady [a,*], Tarek A. Fayed [a], Detlef Gabel [b,1]

[a] *Department of Chemistry, Faculty of Science, University of Tanta, 31527 Tanta, Egypt*
[b] *Department of Chemistry, University of Bremen, P.O. Box 330440, D-28334 Bremen, Germany*

Received 24 November 2007; received in revised form 28 December 2007; accepted 30 December 2007
Available online 8 January 2008

Abstract

Two aza-analogues of distyrylbenzene namely: 1,4-bis[β-(4-quinolyl)vinyl]benzene (PhQ) and 1,4-bis[β-(4-pyridyl)vinyl]benzene (PhPy) containing *arachno*-decaborane or *arachno*-nonaborane clusters have been isolated: 6,9-$(PhQ)_2$-*arachno*-$B_{10}H_{12}$ (**1**), *N*,*N*′-bis[9-Me_2S-*arachno*-$B_{10}H_{12}$-6-yl]PhQ (**2**), 6,9-$(PhPy)_2$-*arachno*-$B_{10}H_{12}$ (**3**), *N*,*N*′-bis[(9-Me_2S)-*arachno*-$B_{10}H_{12}$-6-yl]PhPy (**4**), *N*,*N*′-bis[*arachno*-B_9H_{13}-4-yl]PhQ (**5**), 4-PhQ-*arachno*-B_9H_{13} (**6**), *N*,*N*′-bis[*arachno*-B_9H_{13}-4-yl]PhPy (**7**), and 4-PhPy-*arachno*-B_9H_{13} (**8**). These boronated compounds were easily prepared from the displacement reactions of weaker ligand (SMe_2) of bis (dimethyl sulfide) *arachno*-decaborane(14) {6,9-$(Me)_2SB_{10}H_{12}$}or dimethyl sulfide-*arachno*-nonaborane {4-$(Me)_2SB_9H_{13}$} by the stronger bidentate ligands of PhQ or PhPy in ratio (1:2). The electronic interaction between decaborane or nonaborane *arachno*-type unit and the bonded pyridine units has been investigated by UV–Vis spectroscopy and by AM1 molecular orbital calculations. The resulting compounds undergo *trans–cis* photoisomerization upon excitation. The connection of boron clusters to PhQ and PhPy led to enhancing of the photoreactivity and decreasing of the fluorescence quantum yield of the products.

Keywords: Borane; NMR spectroscopy; MO-calculations; Laser dyes; Aza-distyrylbenzene

1. Introduction

Aza-analogues of distyrylbenzene, e.g. 1,4-bis[β-(4-quinolyl)vinyl]benzene (PhQ) and 1,4-bis[β-(4-pyridyl)vinyl]benzene (PhPy) have been reported as highly efficient blue emitting laser dyes with good photochemical stability (Fig. 1,) [1,2]. Dye lasers are attractive due to their unique feature of tunability over a wide range of wavelengths. Recently, it was reported that PhQ can serve as a probe for biological systems to get information about the site that the probe molecule occupies [3]. The connection of boron clusters to the probes such as PhQ and PhPy may constitute a good entry to generate new fluorescent boron carriers helpful in detecting the accumulation of boron in tumor cells by simple spectrophotometeric methods.

The bis (dimethyl sulfide) adduct of decaborane(14) {6,9-$(Me_2S)_2B_{10}H_{12}$} is one of several compounds that is easily prepared by reacting decaborane ($B_{10}H_{14}$) and a Lewis base [4–6]. The alcoholysis of bis (dimethyl sulfide)-*arachno*-decaborane using methanol led to the formation of dimethyl sulfide-*arachno*-nonaborane {4-$Me_2SB_9H_{13}$} [7]. Both of these borane clusters undergo several interesting reactions [8–15]. The open-faced *arachno* 10 or nine-vertex borane residues will permit tailoring of the borane residues, for example by the addition of metal centers as exemplified by the reaction between {$Co_2(CO)_8$} and the monomer precursor unit {6,9-$(Et_2S)_2B_{10}H_{12}$} to give {$(CO)_6CoB_{10}H_8(Et_2S)_2$} [16]. The reactions of 6,9-$(Me_2S)_2B_{10}H_{12}$ with 4,4′-bipyridyl

* Corresponding author. Tel.: +20 40 3297974; fax: +20 40 3350804.
E-mail address: afafgenady@hotmail.com (A.R. Genady).
[1] Fax: +49 421 2182871.

0022-328X/$ - see front matter © 2008 Elsevier B.V. All rights reserved.
doi:10.1016/j.jorganchem.2007.12.028

and pyrazine (1,4-diazabenzene) resulted in the formation of two potential pyridine-borane oligomer and polymer building blocks and characterized by X-ray single crystal [17].

The molecules prepared in this work were obtained by spontaneous displacement of weaker ligand (SMe_2) from preformed 6,9-$(Me_2S)_2B_{10}H_{12}$ or 4-$Me_2SB_9H_{13}$ by stronger ligands such as PhQ and PhPy. The preparation of these new molecules aims to study the effect of increasing the conjugation path connecting the *arachno* decaborane or nonaborane units. Also, semiempirical AM1 molecular orbital calculations were performed to compare the experimental results with the calculated structures expressed by the UV–Vis spectra. The study is extended to test the photochemical stability of these compounds by determining the percentage of the *cis* isomer formed at the photostationary state upon irradiation.

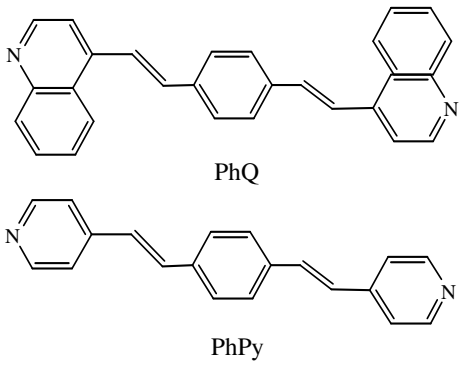

Fig. 1. Structures of aza-distyrylbenzene and their abbreviations.

2. Chemistry of the synthesized compounds

We have found that the exchange of the weak ligand (SMe_2) of 6,9-$(Me_2S)_2B_{10}H_{12}$ or 4-$Me_2SB_9H_{13}$ by another strong ligand such as PhQ or PhPy is a convenient route for the formation of new N-substituted numbers of decaboranes or nonaboranes. Reaction of 6,9-$(Me_2S)_2B_{10}H_{12}$ with PhQ and PhPy in ratios 2:1 in CH_2Cl_2 for one day at room temperature followed by TLC separation gave 6,9-$(PhQ)_2$-*arachno*-$B_{10}H_{12}$ (**1**, faint red color, 32%), *N*, *N*′-bis[9-Me_2S-*arachno*-$B_{10}H_{12}$-6-yl]PhQ (**2**, orange color, 24%) and 6,9-$(PhPy)_2$-*arachno*-$B_{10}H_{12}$ (**3**, faint red color, 28%), *N*,*N*′-bis[(9-Me_2S)-*arachno*-$B_{10}H_{12}$-6-yl]PhPy (**4**, orange color, 25%), respectively (Scheme 1). During the TLC separation of these compounds a variety of orange and red colored components were observed, most of which were unstable in solution, probably because of ligand exchange processes.

Alternatively, the reaction of 4-$Me_2SB_9H_{13}$ with PhQ and PhPy under the same conditions led to the formation of *N*,*N*′-bis[*arachno*-B_9H_{13}-4-yl]PhQ (**5**, red color, 32%), 4-PhQ-*arachno*-B_9H_{13} (**6**, yellow color, 26%), *N*,*N*′-bis-[*arachno*-B_9H_{13}-4-yl]PhPy (**7**, red color, 35%), and 4-PhPy-*arachno*-B_9H_{13} (**8**, yellow color, 24%), respectively (Scheme 2).

All of these compounds were fully characterized by elemental analysis, IR, NMR, UV–Vis, fluorescence, and mass spectrometry (see Section 6). ^{11}B and ^{1}H NMR spectroscopic data of the prepared compounds are listed in

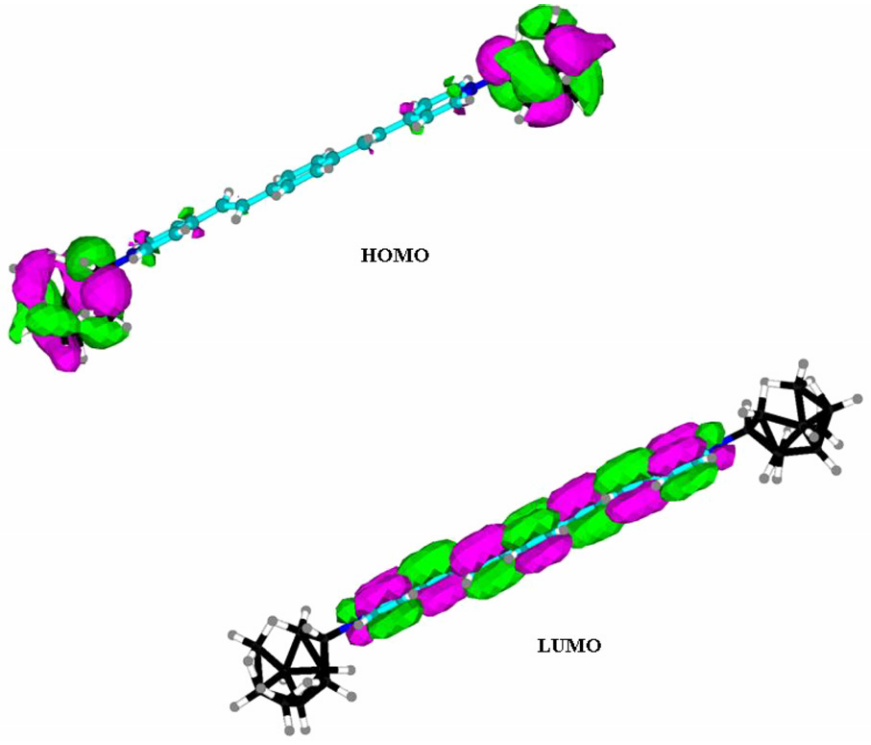

Fig. 2. Representation of optimized HOMO and LUMO levels of compound **7**.

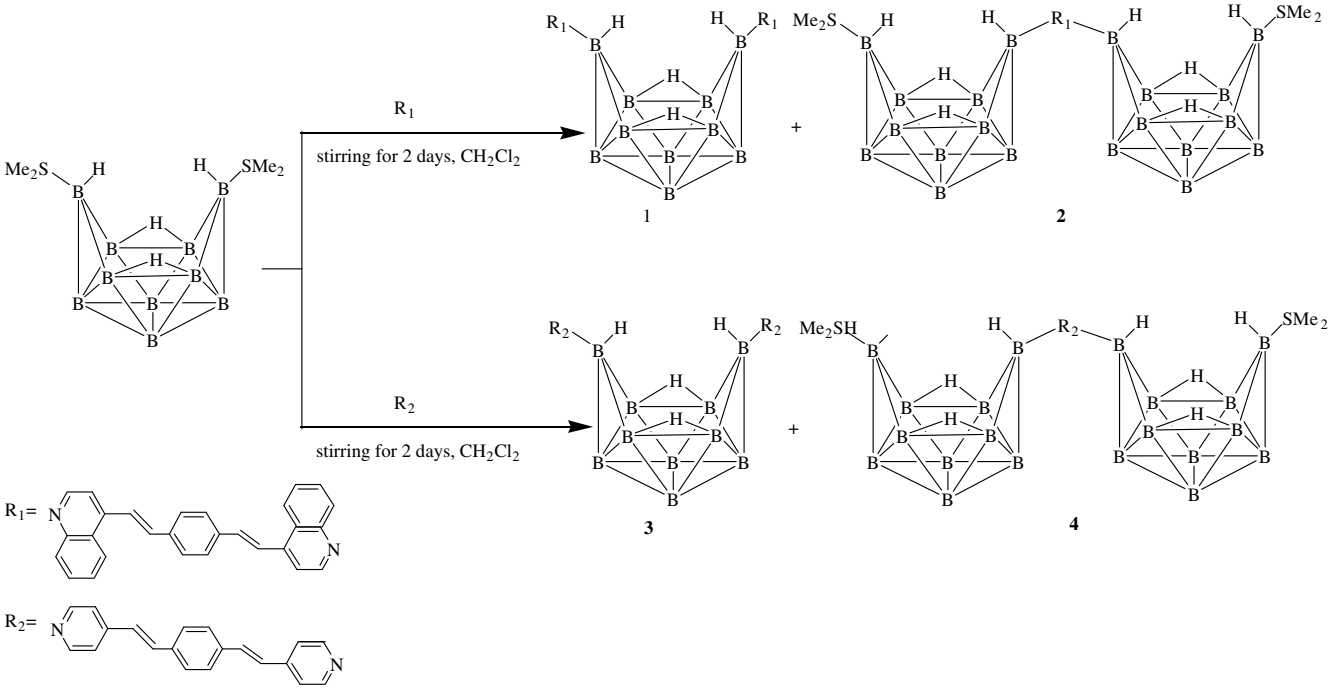

Scheme 1. Exo H atoms are omitted for clarity.

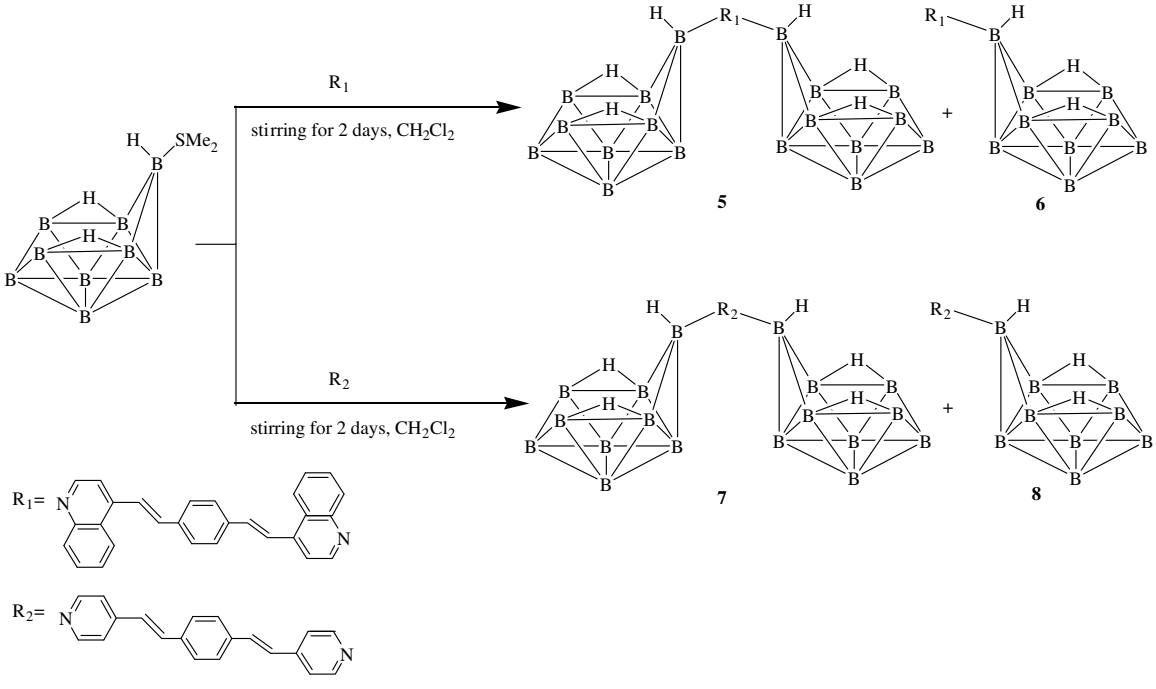

Scheme 2. Exo H atoms are omitted for clarity.

Table 1. As can be seen, there are some minor variations in the proton shielding as the organic moiety of the aza-analogue of distyrylbenzene is changed.

3. Spectral behavior of the synthesized compounds

The electronic interaction between the diolefinic ligands and the boron clusters leads to characteristic spectral changes in the UV–Vis range. The spectral behavior of both free ligands and two of their boronated compounds **2** and **4** has been studied in CH_2Cl_2 and CH_3CN solvents. Fig. 4 shows the steady-state absorption and emission spectra of PhPy and compound **2** in CH_2Cl_2 as an example, while the corresponding data are collected in Table 3. As can be seen, the free ligands exhibit strong absorption around 360 nm (molar absorptivity ranges from 39 500 to

Table 1
200 MHz (^{11}B, ^{1}H) NMR data of boronated dye laser compounds **1**–**8** in CD_3Cl at 20 °C

Compound	B1	B2	B3	B4	B5	B6	B7	B8	B9	B10 μH, *endo*-H
	$\delta(^{11}B)$	$\delta(^{11}B)$	$\delta(^{11}B)$	$\delta(^{11}B)$	$\delta(^{11}B)$	$\delta(^{11}B)$	$\delta(^{11}B)$	$\delta(^{11}B)$	$\delta(^{11}B)$	$\delta(^{11}B)$
	[$\delta(^{1}H)$]	[$\delta(^{1}H)$]	[$\delta(^{1}H)$]	[$\delta(^{1}H)$]	[$\delta(^{1}H)$]	[$\delta(^{1}H)$]	[$\delta(^{1}H)$]	[$\delta(^{1}H)$]	[$\delta(^{1}H)$]	[$\delta(^{1}H)$]
1	−40.24	−3.6	−40.24	−3.6	−19.91	−22.89	−19.91	−19.91	−22.89	−19.91
	[0.39]	[2.28]	[0.39]	[2.28]	[1.59]	[−0.28]	[1.59]	[1.59]	[−0.28]	[1.59], [−4.71]
2[a]	−40.18	−3.43	−40.22	−3.43	−19.97	−23.95	−19.97	−19.97	−23.95	−19.97
	[0.37]	[2.25]	[0.39]	[2.25]	[1.56]	[−0.35]	[1.56]	[1.56]	[−0.33]	[1.56], [−4.68]
3	−40.22	−3.52	−40.24	−3.52	−19.96	−22.96	−19.96	−19.96	−22.96	−19.96
	[0.39]	[2.27]	[0.39]	[2.27]	[1.59]	[−0.29]	[1.59]	[1.59]	[−0.29]	[1.59], [−4.68]
4[a]	−40.25	−3.43	−40.25	−3.43	−19.89	−24.05	−19.89	−19.89	−24.05	−19.89
	[0.4]	[2.27]	[0.4]	[2.27]	[1.54]	[−0.38]	[1.54]	[1.54]	[−0.38]	[1.54], [−4.71]
5[a]	4.52	−39.18	−39.18	−23.64	−16.36	−21.49	18.19	−21.49	−16.36	
	[3.04]	[0.49]	[0.42]	[0.38]	[1.56]	[1.97]	[4.1]	[1.83]	[1.56]	[−3.52], [−0.0018]
6	4.59	−39.15	−39.15	−23.74	−16.35	−21.51	18.20	−21.51	−16.35	
	[3.02]	[0.47]	[0.43]	[0.39]	[1.59]	[1.95]	[4.18]	[1.85]	[1.59]	[−3.51], [−0.0019]
7[a]	4.55	−39.21	−39.21	−23.65	−16.57	−21.55	18.22	−21.55	−16.57	
	[3.07]	[0.48]	[0.42]	[0.36]	[1.53]	[1.89]	[4.05]	[1.79]	[1.53]	[−3.49], [−0.0016]
8	4.49	−39.12	−39.12	−23.18	−16.38	−21.41	18.19	−21.41	−16.38	
	[3.05]	[0.46]	[0.40]	[0.35]	[1.54]	[1.97]	[4.18]	[1.82]	[1.54]	[−3.57], [−0.0018]

[a] All bands were broad.

44 000 M^{-1} cm^{-1} depending on the solvent) and structured fluorescence emission with a good fluorescence quantum yield (about 0.2). The absorption and fluorescence spectral bands of the formed compounds are broad and shifted to longer wavelengths. Also, the fluorescence emission of the products is quenched as indicated by the lower quantum yield ($\phi_f = 0.12$). The fluorescence quenching is accompanied by enhancement of the photoreactivity as reflected by the increase of the percentage of the less stable *cis* isomer (x-*cis*) formed at the photostationary state due to the *trans–cis* photoconversion. Fig. 5 displays the change of the absorption spectra of compound **6** following irradiation at 365 nm using a medium pressure Hg-lamp. Upon irradiation of the solution at room temperature, the absorbance of the band at 375 nm decreases with an increase of the absorption at 275 nm until reaching a photostationary state. These changes are accompanied by the appearance of an isosbestic point, indicating an equilibrium between the *trans* and *cis* forms, and was attributed to the known *trans*/*cis* photoisomerization. The stability of the photostaionary composition under irradiation for longer time (>15 min) as well as appearance of only one isosbestic point indicates the formation of only one photoproduct. This is likely to be the *cis* isomer formed due to the isomerization of only one ethylenic bond as reported previously for the free ligand [2]. The fluorescence spectrum of the irradiated solution suffers a decrease in its intensity without any shift or change in the band profile indicating that the *cis*-isomer of the boronated compound is non-fluorescent. Based on this fact, the extent of *trans–cis* conversion (x-*cis*) was calculated from the fluorescence intensities measured at the emission maximum before and after irradiation (I_f^0 and I_f^{pss}, respectively), using the following equation [20];

$$x - cis = (I_f^0 - I_f^{pss})/I_f^0$$

The value of x-*cis* for compound **6** in CH_2Cl_2 thus calculated is 0.72 which is considerably larger than that

Table 2
Energies of the highest occupied molecular orbital (HOMO) and the lowest unoccupied molecular orbital (LUMO) for the boronated compounds **1**–**8** calculated after geometry optimization at AM1 level

Compound	λ_{max} (nm)	$1/\lambda_{max}$ (10^{-3} cm^{-1})	HOMO (eV)	LUMO (eV)	$\Delta E_{LUMO-HOMO}$ (eV)
1	465	2.15	−7.57	−1.59	5.98
2	401	2.49	−8.07	−0.59	7.48
3	454	2.20	−7.95	−1.72	6.23
4	395	2.53	−8.38	−0.71	7.67
5	452	2.21	−8.66	−2.35	6.31
6	396	2.52	−8.73	−1.14	7.59
7	448	2.23	−8.71	−2.29	6.42
8	398	2.51	−8.67	−1.12	7.55

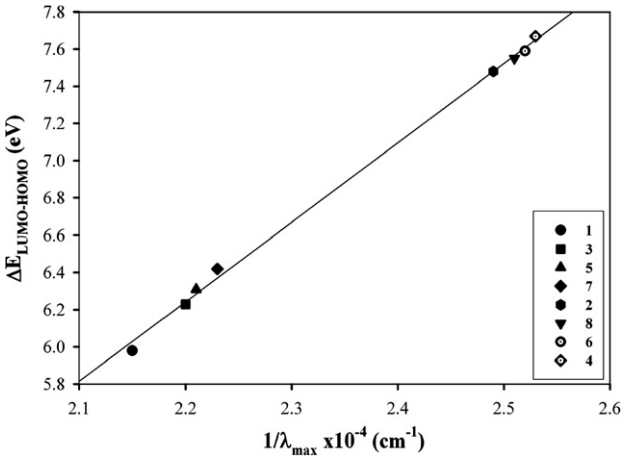

Fig. 3. Correlation of the energy differences $\Delta E_{LUMO-HOMO}$ with $1/\lambda_{max}$ for the boronated compounds **1**–**8**.

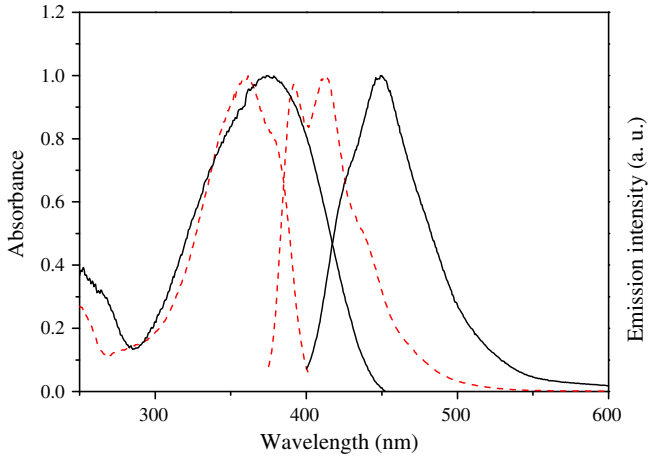

Fig. 4. Normalized absorption and fluorescence emission spectra of 5×10^{-5} M of PhPy (---) and its boronated compound **4** (—) in CH_2Cl_2 at room temperature.

Table 3
Spectral data of 5×10^{-5} M of PhPy, PhQ, and their boronated compounds (**2** and **4**) in CH_2Cl_2 and CH_3CN

Compound	CH_2Cl_2			CH_3CN		
	λ_a (nm)	λ_f (nm)	ϕ_f	λ_a (nm)	λ_f (nm)	ϕ_f
PhPy	361	412,392	0.203	348	410	0.178
4	375	450	0.122	474	450	0.089
PhQ	367	455,432	0.28	370	454	0.147
2	395	477	0.069	384	480	0.051

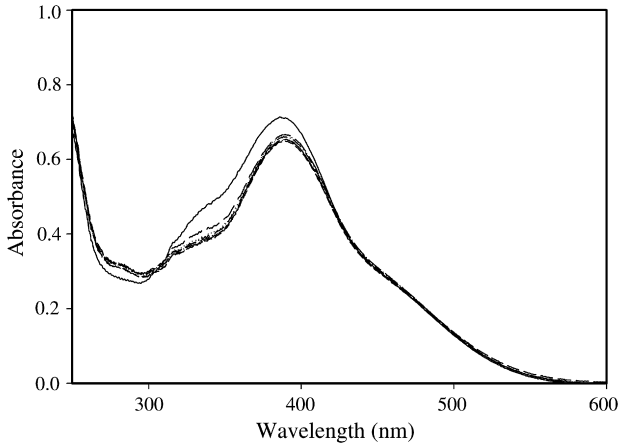

Fig. 5. The absorption spectra of 7×10^{-5} M of compound **6** in CH_2Cl_2 following irradiation at 365 nm using a medium pressure Hg-lamp (time interval = 1 min).

calculated for the free ligand (0.50). In contrast, the absorption spectrum of the corresponding dimeric analogue (compound **5**) displays no changes upon irradiation in CH_2Cl_2 at 365 nm for more than 10 min. This indicates that this compound has a higher photostability, which might be attributed to the steric hindrance caused by the bulky boron clusters on both sides.

4. Molecular orbital calculations

With the aim of explaining the color change of pyridine-*arachno*-borane compounds as part of understanding of this interesting and potentially important type of the compounds, semiempirical AM1 theoretical calculations were performed [18]. This type of calculation gives the HOMO (highest occupied molecular orbital) and LUMO (lowest unoccupied molecular orbital) energies, which we have used for interpretation. We did not use electronic spectra calculations that are only useful for directly comparing measured and calculated spectra, rather than energy-level differences, and which, therefore, do not allow any detailed view on how the substituents may influence the absorption maxima. At an initial empirical level, we were interested in explaining the dependence of the color indicated by the longest wavelength absorption band with respect to the nature of substituent on the pyridine rings. In order to approach this, the AM1 calculations were therefore carried out on the 1,4-bis[β-(4-pyridyl)vinyl]benzene (PhPy) and its 4-quinolyl derivative such as PhQ. The energies of the HOMO and LUMO levels obtained after complete geometry optimization are listed in Table 2 while representation of these orbitals for compound **7** is depicted in Fig. 2.

The differences in energy ($\Delta E_{LUMO-HOMO}$) show a linear correlation with the experimental data for λ_{max} as determined from the UV–Vis absorption spectroscopy (Fig. 3). Analysis of the data in Table 2 reveal that there is only a small change in the HOMO energy, therefore, the correlation of $\Delta E_{LUMO-HOMO}$ with the absorption spectra arises principally from the larger variation in the energy of LUMO. Therefore, it was concluded that the principal elements of molecular orbital structure which are responsible for the color can be constructed qualitatively from combination of fragments of the HOMO at the borane cluster and the π-LUMO of the PhQ or PhPy. The calculated orbital-energy difference are between 5.98 and 7.59 eV which are responsible for the absorption in the visible region. Also, due to the localization of the LUMO level on the complexed pyridine fragment, the color shows a dependence on the pyridine substituents where a π-donor leads to a blue shift, whereas a π-acceptors leads to a red shift.

It has been shown previously that the colors of the 6,9-bis-pyridine-*arachno*-decaborane {6,9-$(C_5H_5N)_2$-*arachno*-$B_{10}H_{12}$} and its ring substituted derivatives vary from a very pale yellow to a deep red, depending on the substituent group on the pyridine ligand [5,19]. In the case of {6,9-$(C_5H_5N)_2$-*arachno*-$B_{10}H_{12}$}and its ring-substituted derivatives, electron-withdrawing substituents also shifted the absorption band at the longest wavelength to the red, whereas a π-donor substitutent led to a blue shift. The differences of the number of boron atoms of the cluster between 10-vertex *arachno* {B_{10}} and 9-vertex *arachno* {B_9} would, therefore, appear to have no significant influence on the color of their pyridine complexes, because the {B_9} series shows very similar colorations to the {B_{10}} series [5,19].

The results of our calculations suggest a strong dependence of the absorption maxima in UV–Vis spectra on the LUMO energy of the substituted pyridines. It seems likely that changes in the rotamer conformation about the B–N(pyridine) vector should not have a strong influence on the LUMO of the pyridine moiety and therefore on the absorption maxima. Further calculations, especially of the dependence of the rotational barrier about the B–N(pyridine) vector, are needed to test this hypothesis.

5. Conclusion

In conclusion, we have synthesized and characterized novel fluorescent boronated aza-distyrylbenzene derivatives. The presence of weak displacement ligands such SMe_2 group make compounds **2** and **4** are versatile starting material to the synthesis of a wide variety of boron-containing species. For example, further structural modification could make the structures of compounds **2** and **4** especially attractive in the context of supramolecular assemblies [17]. The spectroscopic data of the boronated aza-distyrylbenzene derivatives and the molecular orbital calculations were obtained. The presence of the two cluster units led to a red shift in UV–Vis spectra compared with that containing only one cluster unit. The resulting compounds especially, containing one cluster unit undergo *trans–cis* photoisomerization upon excitation. The connection of boron clusters to PhQ and PhPy enhanced the photoreactivity and decreased the fluorescence quantum yield of the products.

6. Experimental

6.1. Materials and methods

The diolefinic ligands PhQ and PhPy were prepared and characterized as described previously [2]. Steady-state absorption and emission spectral measurements were carried out using a Shimadzu UV-3101PC scanning spectrophotometer and a Perkin–Elmer LS 50B spectrofluorometer, respectively. The samples were excited at 365 nm while recording the fluorescence spectra. The fluorescence quantum yields (ϕ_f) were measured using 9,10-diphenylanthracene as a standard ($\phi_f = 0.96$) (optical densities at the excitation wavelength is less than 0.2) [21]. 6,9-$(Me_2S)_2B_{10}H_{12}$ and 4-$Me_2SB_9H_{13}$ were prepared by literature methods [4–7] and all other reagents were obtained commercially. Reactions were carried out in dry solvents under dry nitrogen but subsequent manipulation and separation procedures were carried out in open air. Preparative thin layer chromatography (TLC) was carried out using 0.75 mm layers of silica gel G (Merck, GF_{254}) made from water slurries on glass plates of dimensions $20 \times 20\ cm^2$, followed by drying in air at 100 °C. Elemental analyses were performed by a Perkin–Elmer 2400 automatic elemental analyzer. All compounds gave elemental analysis within ±0.4%. The measurements for NMR (^{11}B, ^1H and ^{13}C) were carried out on a Bruker DPX 200 spectrometer. The chemical shifts δ are given in ppm relative to $\Xi = 100$ MHz for δ (^1H) (nominally $SiMe_4$), $\Xi = 50$ MHz for δ (^{13}C) (nominally $SiMe_4$), and $\Xi = 32.083$ MHz for δ (^{11}B) (nominally F_3BOEt_2) in CD_3Cl. IR (cm^{-1}) spectra were determined as KBr disc on a Biorad FTS-7 spectrometer. Electron spray ionization (ESI) mass spectra were recorded on a Bruker Esquire in CH_3OH. Only the signal with the highest intensity of the boron isotopic pattern is listed. Molecular-orbital calculations [18] were carried out with HYPERCHEM [22].

6.2. General procedure for preparation of compounds *1–8*

A solution of 6,9-$(Me_2S)_2B_{10}H_{12}$ or 4-$Me_2SB_9H_{13}$, (2.0 mmol) was added to a solution of phenylene-1,4-diethylene-bis-4-quinoline (PhQ) or its 4-pyridyl derivative (PhPy) (1.0 mmol) in 10 ml of dry CH_2Cl_2. The reaction was stirred for two days at room temperature then the solution was filtered off. All volatile components of the filtrate were removed under vacuum at room temperature and the resulting substance was chromatographed on silica gel using CH_2Cl_2 as eluent to yield a variety of orange and red components.

6.2.1. Compound *1*: (Yield: 32%, 152 mg, faint red color, $R_f = 0.25$)

^1H NMR ($CDCl_3$): δ 6.75 (d, $J = 5.0$ Hz, 4 H, CH_{phenyl}), 7.08 (d, $J = 7.0$ Hz, 4H, $CH{=}CH_{aliphatic}$), 7.16 (d,$J = 8.0$ Hz, 8H, CH_{phenyl}), 7.27 (d, $J = 8.0$ Hz, 4H, $CH{=}CH_{aliphatic}$), 7.32 (d, $J = 7.0$ Hz, 4H, $CH{=}CH_{pyridine}$), 7.54 (d, $J = 6.5$ Hz, 4H, CH_{phenyl}), 7.68 (d, $J = 6.5$ Hz, 4H, CH_{phenyl}), 8.5 (d, $J = 7.0$ Hz, 4H, CH_{phenyl}), 8.70 (d, $J = 5.0$ Hz, 2H, $CH{=}N_{pyridine}$), 8.91 (d, $J = 7.0$ Hz, 2H, $CH{=}N_{pyridine}$); ^{13}C NMR ($CDCl_3$): 117.74 ($2CH_{pyridine}$), 121.28, 121.68 ($2CH_{pyridine}$), 124.42, 125.83, 128.05, 128.63 ($20CH_{phenyl}$), 129.05 (4CH=CH), 130.12, 131.25 ($8CH_{phenyl}$), 132.57, 133.56 ($4C_{phenyl}$), 135.34, 137.56 (4CH= CH),146.68, 147.45 (4C=N), 149.12 (4CH=N), 150.62 ($4C_{pyridine}$); MS (ESI): m/z: 890 ($[M]^+$, 57%); IR ν_{max} (KBr disc)/cm^{-1}: 2516s (BH), 1619s (C=C), 1452s (BN),1151s (C–N). Anal. Calc. $B_{10}C_{56}H_{52}N_4$ requires: C, 75.65; H, 5.89; N, 6.3. Found: C, 75.43; H, 5.61; N, 6.13%.

6.2.2. Compound *2*: (Yield: 24%, 12 mg, orange color, $R_f = 0.31$)

^1H NMR ($CDCl_3$): δ 2.54 (s, 12H, SMe_2), 6.72 (d, $J = 7.0$ Hz, 2H, $CH{=}CH_{aliphatic}$), 7.08 (d, $J = 5.0$ Hz, 2H, CH_{phenyl}), 7.24 (d, $J = 6.0$ Hz, 2H, CH_{phenyl}), 7.32 (d, $J = 4.5$ Hz, 2H, $CH{=}CH_{aliphatic}$), 7.45 (d, $J = 6.5$ Hz, 2H, $CH_{pyridine}$), 7.59–7.74 (m, 6H, CH_{phenyl}), 8.53 (d, $J = 7.0$ Hz, 2H, CH_{phenyl}), 8.93 (d, $J = 6.0$ Hz, 2H, $CH{=}N_{pyridine}$); ^{13}C NMR ($CDCl_3$): 27.22, 27.36 (SMe_2), 117.56 ($2CH_{pyridine}$), 122.19, 122.98 ($2CH_{phenyl}$), 125.83, 126.12 ($2C_{phenyl}$), 127.02, 127.31 ($6CH_{phenyl}$), 127.64 ($2CH_{aliphatic}$), 128.47, 131.97 ($4CH_{phenyl}$), 137.41, 138.04 ($2C_{phenyl}$), 145.21, 147.16 (2C=N), 150.51 (2CH=N),

152.21 ($2C_{pyridine}$); MS (ESI): *m/z*: 752 ($[M]^+$, 43%); IR ν_{max}(KBr disc)/cm^{-1}: 1032, 993, 968 (SMe_2), 2533s (BH), 1618s (C=C), 1465s (BN),1149s (CN). Anal. Calc. for $B_{20}C_{32}H_{56}N_2S_2$ requires: C, 51.30; H, 7.53; N, 3.74. Found: C, 51.03; H, 7.16; N, 3.47%.

*6.2.3. Compound **3**: (Yield: 28%, 181 mg, faint red color, $R_f = 0.23$)*

^{1}H NMR ($CDCl_3$): δ 7.17 (d, $J = 8.0$ Hz, 4H, $CH{=}CH_{aliphatic}$), 7.27 (d, $J = 7.0$ Hz, 8H, $CH{=}CH_{phenyl}$), 7.68 (d, $J = 8.0$ Hz, 8H, $CH{=}CH_{pyridine}$), 8.02 (d, $J = 8.0$ Hz, 4H, $CH{=}CH_{aliphatic}$), 8.79 (d, $J = 7.0$ Hz, 4H, $CH{=}N_{pyridine}$), 8.91 (d, $J = 7.0$ Hz, 4H, $CH{=}N_{pyridine}$); ^{13}C NMR ($CDCl_3$): 121.16, 121.98 ($8CH_{pyridine}$), 123.96, 125.38 ($8CH_{phenyl}$), 129.72 (4CH=CH), 131.47 (4CH=CH), 136.54, 137.05 ($4C_{phenyl}$), 145.46, 146.17 ($4C_{pyridine}$), 152.87, 153.12 (8CH=N); MS (ESI): *m/z*: 670 ($[M]^+$, 61%); IR ν_{max}(KBr disc)/cm^{-1}: 2521s (BH), 1624s (C=C), 1459s (BN),1145s (C–N). Anal. Calc. for $B_{10}C_{40}H_{44}N_4$ requires: C, 69.74; H, 6.44; N, 8.13. Found: C, 69.49; H, 6.15; N, 7.86%.

*6.2.4. Compound **4**: (Yield: 25%, 142 mg, orange color, $R_f = 0.37$)*

^{1}H NMR ($CDCl_3$): δ 2.42 (s, 12H, SMe_2), 7.01 (d, $J = 9.0$ Hz, 2H, $CH{=}CH_{aliphatic}$), 7.23 (d, $J = 2.0$ Hz, 4H, $CH{=}CH_{phenyl}$), 7.32–7.41 (m, 4H, $CH{=}CH_{pyridine}$), 8.01 (d, $J = 6.0$ Hz, 2H, $CH{=}CH_{aliphatic}$), 8.55–8.82 (m, 4H, CH=N); ^{13}C NMR ($CDCl_3$): 27.3, 27.58 (SMe_2), 121.95, 122.47 ($4CH_{pyridine}$), 124.87, 125.94 ($4CH_{phenyl}$), 128.65, 129.03, 131.98, 132.67 (4CH=CH), 136.86, 137.27 ($2C_{phenyl}$), 144.54, 146.65 ($2C_{pyridine}$), 151.35, 151.92 (4CH=N); MS (ESI): *m/z*: 652 ($[M]^+$, 39%); IR ν_{max}(KBr disc)/cm^{-1}: 1035s, 993s, 984 (SMe_2), 2525s (BH), 1618s (C=C), 1448s (BN),1162s (C–N). Anal. Calc. for $B_{20}C_{24}H_{52}N_2S_2$ requires: C, 44.41; H, 8.08; N, 4.32. Found: C, 44.18; H, 7.79; N, 4.02%.

*6.2.5. Compound **5**: (Yield: 32%, 231 mg, orange color, $R_f = 0.29$)*

^{1}H NMR ($CDCl_3$): δ 7.07 (d, $J = 4.0$ Hz, 2H, CH_{phenyl}), 7.09 (d, $J = 4.7$ Hz, 2H, $CH{=}CH_{aliphatic}$), 7.21 (d,$J = 6.0$ Hz, 4H, CH_{phenyl}), 7.23 (d, $J = 4.5$ Hz, 2H, $CH{=}CH_{aliphatic}$), 7.33 (d, $J = 5.4$ Hz, 2H, $CH{=}CH_{pyridine}$) 7.51 (d, $J = 7.5$ Hz, 2H, CH_{phenyl}), 7.71 (d, $J = 4.0$ Hz, 2H, CH_{phenyl}), 8.51 (d, $J = 3.8$ Hz, 2H, CH_{phenyl}), 8.92 (d, $J = 7.0$ Hz, 2H, $CH{=}N_{pyridine}$); ^{13}C NMR ($CDCl_3$): 117.19, 121.52, ($2CH_{pyridine}$), 122.27, 125.04, 126.01, 127.93, 128.56 ($10CH_{phenyl}$), 129.42 (2CH=CH), 130.24, 131.05 ($4CH_{phenyl}$), 132.61, 135.89 ($2C_{phenyl}$), 136.46, 137.15 (2CH=CH), 144.92 (2C=N), 147.78 (2CH=N), 152.32 ($2C_{pyridine}$); MS (ESI): *m/z*: 608 ($[M]^+$, 37%); IR ν_{max}(KBr disc)/cm^{-1}: 2525s (BH), 1631s (C=C), 1457s (BN),1153s (C–N). Anal. Calc. for $B_{18}C_{28}H_{46}N_2$ requires: C, 55.56; H, 7.66; N, 4.63. Found: C, 55.21; H, 7.31; N, 4.31%.

*6.2.6. Compound **6**: (Yield: 26%, 182 mg, yellow color, $R_f = 0.22$)*

^{1}H NMR ($CDCl_3$): δ 6.92 (d, $J = 6.4$ Hz, 2H, $CH{=}CH_{aliphatic}$), 7.05 (d, $J = 3.7$ Hz, 2H, CH_{phenyl}), 7.19 (d, $J = 5.5$ Hz, 2H, CH_{phenyl}), 7.24 (d, $J = 3.5$ Hz, 2H, $CH{=}CH_{aliphatic}$), 7.32 (d, $J = 7.0$ Hz, 2H, $CH_{pyridine}$), 7.49–7.65 (m, 6H, CH_{phenyl}), 8.49 (d, $J = 5.0$ Hz, 2H, CH_{phenyl}), 8.94 (d, $J = 3.0$ Hz, 2H, $CH{=}N_{pyridine}$); ^{13}C NMR ($CDCl_3$): 117.35 ($2CH_{pyridine}$), 121.55, 122.65 ($2CH_{phenyl}$), 125.07, 126.52 ($2C_{phenyl}$), 127.18, 127.72, 128.46 ($6CH_{phenyl}$), 129.23 ($2CH_{aliphatic}$), 130.67 132.62 ($4CH_{phenyl}$), 135.84, 136.95 ($2C_{phenyl}$), 143.96, 147.97 (2C=N), 149.56, 150.36 (2CH=N), 152.78, 153.11 ($2C_{pyridine}$); MS (ESI): *m/z*: 496 ($[M]^+$, 52%); IR ν_{max}(KBr disc)/cm^{-1}: 2526s (BH), 1633s (C=C), 1455s (BN),1157s (C–N). Anal. Calc. for $B_9C_{28}H_{33}N_2$ requires: C, 67.96; H, 6.72; N, 5.66. Found: C, 67.71; H, 6.36; N, 5.41%.

*6.2.7. Compound **7**: (Yield: 35%, 196 mg, orange color, $R_f = 0.34$)*

^{1}H NMR ($CDCl_3$): δ 7.0 (d, $J = 5.0$ Hz, 2H, $CH{=}CH_{aliphatic}$), 7.20 (d, $J = 3.0$ Hz, 4H, $CH{=}CH_{phenyl}$), 7.29–7.38 (m, 4H, $CH{=}CH_{pyridine}$), 7.98 (d, $J = 4.0$ Hz, 2H, $CH{=}CH_{aliphatic}$), 8.56–8.93 (m, 4H, CH=N); ^{13}C NMR ($CDCl_3$):121.54, 122.21 ($4CH_{pyridine}$), 123.87, 124.98 ($4CH_{phenyl}$), 127.25, 128.34, 131.45, 132.47 (4CH=CH), 136.12, 137.65 ($2C_{phenyl}$), 145.21, 146.99 ($2C_{pyridine}$), 151.67, 151.98 (4CH=N); MS (ESI): *m/z*: 508 ($[M]^+$, 32%); IR ν_{max}(KBr disc)/cm^{-1}: 2526s (BH), 1627s (C=C), 1451s (BN),1158s (C–N). Anal. Calc. for $B_{18}C_{20}H_{42}N_2$ requires: C, 47.55; H, 8.38; N, 5.55. Found: C, 47.37; H, 8.04; N, 5.27%.

*6.2.8. Compound **8**: (Yield: 24%, 157 mg, yellow color, $R_f = 0.21$)*

^{1}H NMR ($CDCl_3$): δ 7.01 (d, $J = 7.0$ Hz, 2H, $CH{=}CH_{aliphatic}$), 7.18 (d, $J = 6.3$ Hz, 4H, $CH{=}CH_{phenyl}$), 7.29–7.38 (m, 4H, $CH{=}CH_{pyridine}$), 8.04 (d, $J = 4.0$ Hz, 2H, $CH{=}CH_{aliphatic}$), 8.55 (d, $J = 5.0$ Hz, 2H, CH=N), 8.92 (d, $J = 3.0$ Hz, 2H, CH=N); ^{13}C NMR ($CDCl_3$): 121.44, 122.26 ($4CH_{pyridine}$), 123.76, 124.99 ($4CH_{phenyl}$), 127.45, 128.63, 131.79, 132.52 (4CH=CH), 136.24, 137.55 ($2C_{phenyl}$), 145.32, 146.87 ($2C_{pyridine}$), 151.74, 152.17 (4CH=N); MS (ESI): *m/z*: 396 ($[M]^+$, 29%); IR ν_{max}(KBr disc)/cm^{-1}: 2528s (BH), 1624s (C=C), 1456s (BN),1156s (C–N). Anal. Calc. for $B_9C_{20}H_{29}N_2$ requires: C, 60.85; H, 7.4; N, 7.10. Found: C, 60.51; H, 7.12; N, 6.89%.

Acknowledgement

The authors are grateful to Dr. Tobias Borrmann, Department of Chemistry, University of Bremen, Germany, for helping us in the MO-calculations.

References

[1] E.M. Ebeid, M.M.F. Sabry, S.A. El-Daly, Laser Chem. 5 (1985) 223.

[2] S.A. El-Daly, T.A. Fayed, Spectrochim. Acta A 55 (1999) 2579.
[3] T.A. Fayed, S.H. Etaiw, S. Landgraf, G. Grampp, Photochem. Photobiol. Sci. 2 (2003) 376.
[4] R. Schaeffer, J. Am. Chem. Soc. 79 (1957) 1006.
[5] B.M. Graybill, M.F. Hawthorne, J. Am. Chem. Soc. 83 (1961) 2673.
[6] C. Naar-Colin, T.L. Heying, Inorg. Chem. 2 (1963) 659.
[7] B.M. Graybill, J.K. Ruff, M.F. Hawthorne, J. Am. Chem. Soc. 83 (1961) 2669.
[8] X.L.R. Fontaine, J.D. Kennedy, J. Chem. Soc., Dalton Trans. (1998) 441.
[9] D.F. Gaines, Inorg. Chem. 39 (2000) 1812.
[10] K.L.F. Callaghan, U. Dörfler, T.D. McGrath, M. Thornton-Pett, J.D. Kennedy, J Organomet. Chem. 550 (1998) 441.
[11] M. Roth, P. Paetzold, Chem. Ber. 128 (1995) 1221.
[12] M.E. El-Zaria, U. Dörfler, D. Gabel, Angew. Chem., Int. Ed. Engl. 41 (2002) 4498.
[13] M.E. El-Zaria, U. Dörfler, D. Gabel, J. Med. Chem. 45 (2002) 5817.
[14] M.E. El-Zaria, A.R. Genady, D. Gabel, Chem. Eur. J. 12 (2006) 8084.
[15] A.K. Bandyopadhyaya, S. Narayanasamy, R.F. Barth, W. Tjarks, Tetrahedron Lett. 48 (2007) 4467.
[16] D.M. Schubert, C.B. Knobler, P.A. Wegner, M.F. Hawthorne, J. Am. Chem. Soc. 110 (1988) 5219.
[17] M.G.S. Londesborough, C. Price, M. Thornton-Pett, W. Clegg, J.D. Kennedy, Inorg. Chem. Commun. 2 (1999) 298.
[18] J.J.P. Stewart, J. Comp. Aided Molec. Des. 4 (1990) 1.
[19] T. Schaefer, R. Sebastian, R. Salman, Can. J. Chem. 59 (1981) 3026.
[20] G. Gauglitz, R. Goes, W. Stooss, R. Raue, Z. Naturforsch. 406 (1985) 317.
[21] J.V. Morris, M.A. Mahaney, J.R. Huber, J. Phys. Chem. 80 (1976) 969.
[22] HYPERCHEM 5.1, HyperCube Inc., Waterloo, Ontario Canada.